Volume 61
Number 83
25 October 2025
Pages 16109–16292

ChemComm

Chemical Communications

rsc.li/chemcomm

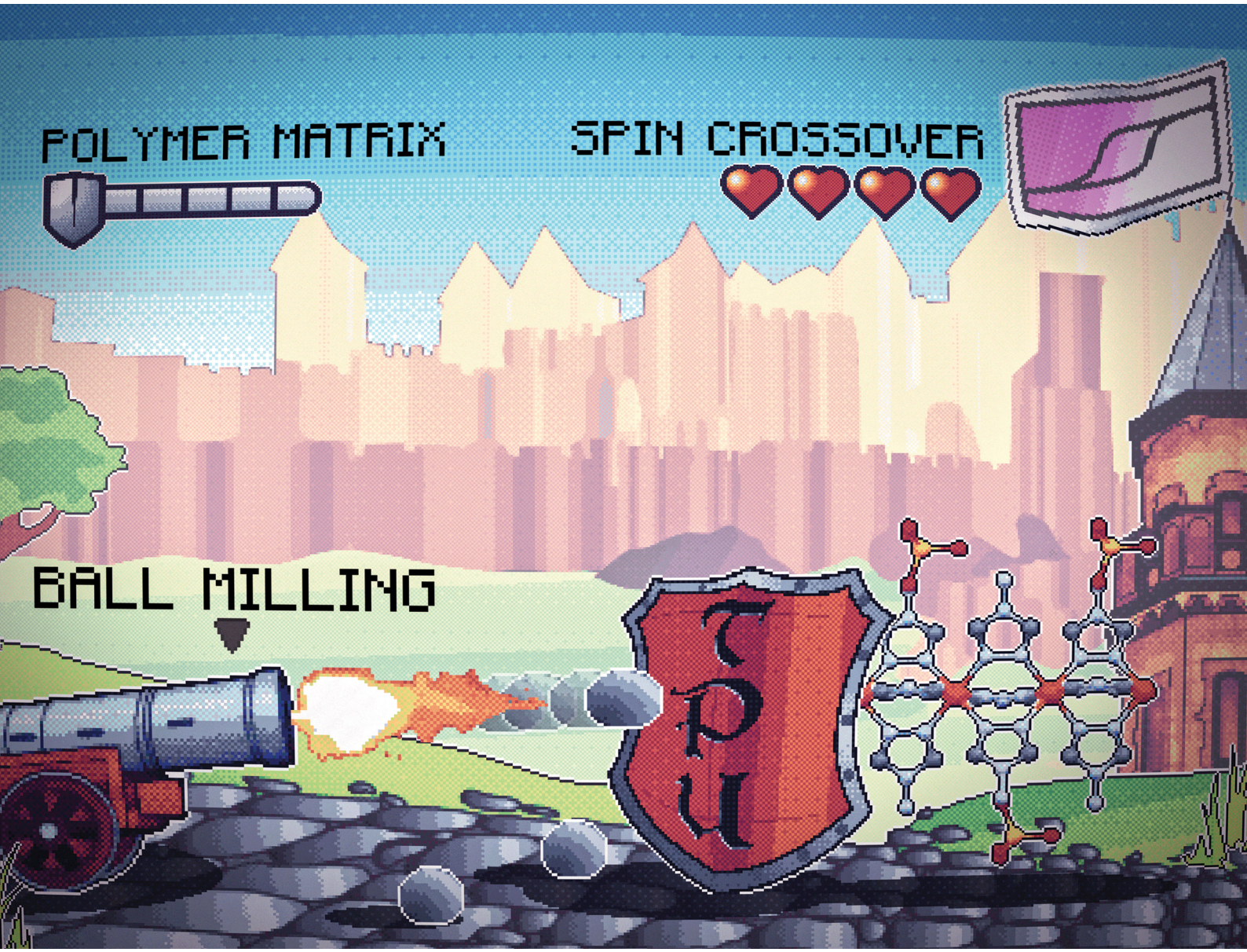

ISSN 1359-7345

ROYAL SOCIETY OF CHEMISTRY

COMMUNICATION

Lionel Salmon, Azzedine Bousseksou *et al.*
Spin crossover particle shielding upon grinding in thermoplastic polyurethane composites

ChemComm

COMMUNICATION

View Article Online
View Journal | View Issue

Cite this: *Chem. Commun.*, 2025, **61**, 16190

Received 24th July 2025,
Accepted 3rd September 2025

DOI: 10.1039/d5cc04205d

rsc.li/chemcomm

Spin crossover particle shielding upon grinding in thermoplastic polyurethane composites

Adelais Trapali, Jean-François Meunier, Michel Baltas, Lionel Salmon * and Azzedine Bousseksou*

Ball milling experiments were conducted on spin crossover (SCO) powder and SCO@polyurethane composite samples. The study reveals that the presence of the TPU matrix acts as a shield for the SCO particles upon grinding, precluding their deactivation. This result is encouraging for the integration of SCO materials into devices.

Nowadays, many research groups are working on the application of coordination compounds in various fields such as therapeutic agents, catalysts, environmental chemicals and smart materials.[1–4] Among the later class of compounds, spin crossover (SCO) complexes are promising candidates for their implementation as active elements in optical, electrical and mechanical devices.[5–8] This singularity which corresponds to an intramolecular electron transfer occurring in between 3d metal orbitals triggered by various stimuli (light, temperature, guest, ...) can be considered as a reversible and robust phenomenon.[9,10] In particular, it has been shown that these compounds, whether in the solid state or integrated into devices, can be subjected to numerous thermal cycles without any clear degradation of their physical properties.[11–14] Nevertheless, the consequent intrinsic breathing of the metal coordination sphere and/or external perturbations can alter the crystal structure and the microstructure, which usually lead to the narrowing of the hysteresis loop when present as well as more gradual and less complete spin transitions. In particular, it has been shown for nanocrystalline powder samples and by detailed crystallographic[15] and atomic force microscopy (AFM)[16] studies that in some cases, the fatigability of the SCO properties can be attributed to the evolution of the lattice and microstructural properties.

On the other hand, several experiments have shown that grinding, milling and other mechanical treatments of solid compounds can lead to significant degradation of the transition curves exhibiting less cooperative behavior and increased residual high spin (HS) or low spin (LS) fractions.[17–24] In fact, the grinding procedure leads to an increase in the number of crystal defects, which multiply the number of nucleation sites influencing the width and the flattening of the hysteresis loop. Moreover, the spin transition has been found to be fully suppressed for certain compounds ground by ball milling.[17] It is interesting to notice also that synthetic and post-synthetic grinding can be used to access new polymorphs/materials that have not previously been isolated using more conventional solution-state techniques.[25–27] Although similar features were obtained on comparing grinding and pressure effects of *ca.* 1.5 kbar on the same powder sample,[22] in general pressure gives rise to specific alteration.[28] The effect of a change in the external pressure has been widely studied and the main effect is the stabilization of the low spin state, *i.e.* the increase of the transition temperature following the Clausius–Clapeyron equation.[29–32] This can be interpreted in terms of the volume reduction, which accompanies the HS to LS change, arising from the shorter metal–ligand donor atom distances in the LS state; an increase in pressure favoring the small-volume LS state. A few opposite cases for which the HS state is stabilized have also been reported and arise because of the alteration of the crystal structure by the applied pressure.[33] To go toward applications using SCO materials, one of the main strategies is to integrate SCO-based nanoparticles[34] into polymers to form nanocomposite films or devices;[35–38] the reduced size of the filler part arising rather homogeneous composite materials. The choice of different classes of polymers and/or the integration of a combination of various types of filler can also generate multifunctional polymer composites (thermally and electrically conductive, mechanically reinforced, flexible...).[37,38] Moreover, it has been shown that specific polymers can be used as a protective element to maintain the SCO properties with respect to external perturbations.[39] On the other hand, matrix effects influencing the SCO properties of the filler have also been reported.[40–42]

In this context, we report hereafter the comparison of the effect of ball milling on SCO particle-based powder and thermoplastic polyurethane (TPU)-based composite samples. X-ray powder diffraction, calorimetry and magnetic measurements

LCC, CNRS & Université de Toulouse (UPS, INP), 31077 Toulouse, France. E-mail: lionel.salmon@lcc-toulouse.fr, azzedine.bousseksou@lcc-toulouse.fr

as well as transmission electron microscopy are implemented to probe if the presence of the polymer can act as protection to preclude the alteration of the SCO properties upon grinding.

Samples were ball milled using a RETSCH MM400 grinding machine equipped with a stainless steel screw-lock jar of 10 mL containing 2 stainless steel 7 mm-diameter balls. Grinding was carried out at 30 Hz by increasing the time up to 20 minutes. Powder X-ray diffraction patterns were recorded using a PANalytical X'Pert equipped with a Cu X-ray tube, a Ge(111) incident beam monochromator (λ = 1.5406 Å) and an X'Celerator detector. Differential scanning calorimetry (DSC) measurements were conducted using a Netsch DSC 3500 Sirius instrument under a nitrogen purging gas flow (20 mL min^{-1}) at a heating/cooling rate of 10 °C min^{-1}. Variable-temperature magnetic susceptibility data were obtained at cooling and heating rates of 2 °C min^{-1} under a field of 0.1 T using a Quantum Design MPMS magnetometer. The experimental data were corrected for the diamagnetic contribution. Zero-field ^{57}Fe Mössbauer spectra were recorded at 290 K using a conventional constant-acceleration type spectrometer equipped with a 50 mCi ^{57}Co source. Least-square fittings of the Mössbauer spectra were applied with the assumption of Lorentzian line shapes. The size and morphology of the samples were determined by transmission electron microscopy (TEM) using a JEOL JEM-1400. TEM samples were prepared by placing a drop of the particles (suspended in ethanol) on a carbon-coated copper grid.

All reagents were purchased from Sigma Aldrich and used without further purification. TPU85A was supplied by BASF. $[Fe(NH_2trz)_3](SO_4)$ bulk powder sample was synthesized according to ref. 12 and the corresponding $[Fe(NH_2trz)_3](SO_4)$@TPU composite film including 20 wt% SCO was obtained by blade casting following the procedure reported in ref. 38. The thickness of the resulting film containing SCO particles is about 70 microns measured by a Mitutoyo micrometer. Before ball milling, the film was preliminarily manually cut to obtain plaquettes of *ca.* 5 mm side. Thermogravimetric analyses reported in Fig. S1 show the similar thermal stability up to 400 K for selected samples.

As illustrated in Fig. 1, powder $[Fe(NH_2trz)_3](SO_4)$ samples and pieces of composite $[Fe(NH_2trz)_3](SO_4)$@TPU films were ball milled at liquid nitrogen temperature during increasing time from 2 to 20 minutes. Photos gathered in Fig. 1 show the starting and after 20 min grinding for both types of samples. Among SCO complexes, the $[Fe(NH_2trz)_3](SO_4)$ compound was selected for its thermal cycling stability and its transition temperatures above room temperature, which makes it attractive for real applications.

To probe and compare the effect of the grinding on the SCO properties of the samples, both DSC and magnetic measurements were performed as a function of temperature. Plots corresponding to the second thermal cycles for each sample and for increasing grinding time are reported in Fig. 2, from which the extracted data are gathered in Table 1. Concerning the DSC data shown in Fig. 2 and for the starting materials, peaks around 55 and 70 °C for the cooling and heating mode, respectively, can be clearly associated with the transition temperature of the complex.

From these peaks we can extract the enthalpy variation (ΔH) of *ca.* 55 J g^{-1}, which reveals a complete transition of the molecules from the LS to the HS state and *vice versa*. In agreement with the powder X-ray diffraction results hereafter, the broadening of the peak for the composite sample can be due to the presence of the polymer.

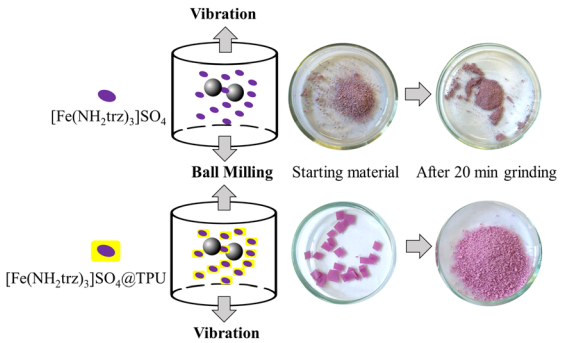

Fig. 1 Scheme illustrating the ball milling experiments for powder and composite samples and the corresponding picture before and after 20 minutes ball milling.

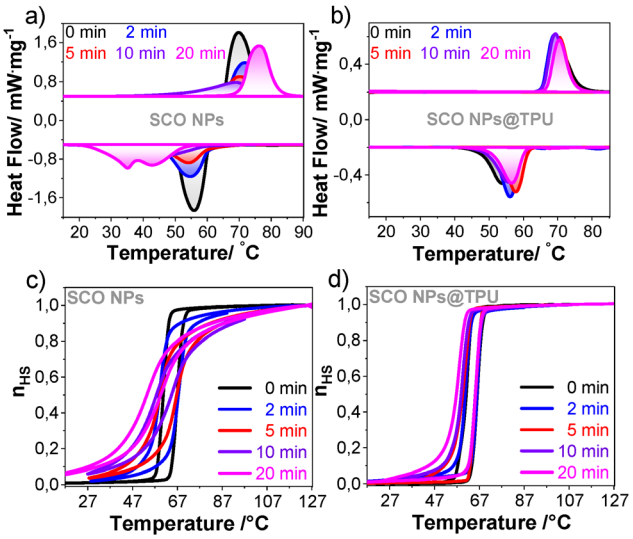

Fig. 2 Differential scanning calorimetry and normalized magnetic measurements for the different samples.

Table 1 Enthalpy variation and SCO properties estimated from DSC and magnetic measurements, respectively (*corrected by the SCO complex fraction in the composite), for different grinding times

Sample	ΔH	$T_{1/2\downarrow}$	$T_{1/2\uparrow}$	n_{HS} at RT
NPs 0 min	56	61	67	0
NPs 2 min	41	59	67	0.02
NPs 5 min	28	58	65	0.03
NPs 10 min	28	54	61	0.05
NPs 20 min	—	50	56	0.08
NPs@TPU 0 min	55*	61	66	0
NPs@TPU 2 min	61*	61	66	0
NPs@TPU 5 min	58*	60	66	0
NPs@TPU 10 min	56*	60	65	0
NPs@TPU 20 min	54*	58	65	0

While the evolution of the peak for the composite sample upon increasing the grinding time is not significant with a nearly constant ΔH, the same conclusion cannot be drawn for the ground powder sample. Indeed, for the later one, larger thermal shift of the peak associated with a clear broadening and splitting can be observed. Such observations are also reflected by the decrease of ΔH pointing out the modification of the complex and/or the generation of defects in the coordination network.

Variable temperature magnetic measurements were also conducted on the SCO NPs and SCO NPs@TPU composite samples between 25 °C and 100 °C, with a temperature ramp of 2 °C per minute (Fig. 2c and d). Two thermal cycles were performed for each sample, but only the second cycle is considered here, as the first cycle usually involves irreversible structural reorganization and solvent loss. From the normalized curves (using Mössbauer data), we can extract the transition temperature defined as the temperature for which the proportions of LS and HS molecules are equal ($n_{HS} = 0.5$) in the cooling ($T_{1/2\downarrow}$) and heating ($T_{1/2\uparrow}$) modes and the estimated residual fraction of HS molecules at 25 °C. It is interesting to notice that the diamagnetic correction of the ligands and the TPU matrix as well as the proportion of the iron complex have been considered in the treatment of the data. Moreover, Mössbauer measurements carried out at 290 K confirm the absence of HS residual fraction at low temperature for the ground composite films (see Fig. S2). In a similar way, we can conclude that the effect of the grinding on the composite sample can be neglected; only a slight decrease of the cooperativity can be observed. On the other hand, a clear evolution of the plot upon increasing the grinding time can be highlighted for the particle-based samples. After only 2 minutes, the transition temperatures and the cooperativity decrease, while a residual fraction of HS species appears, and all these effects increase with milling time. The residual HS fraction corresponding to the damaged/inactive SCO molecules after 20 minutes ball milling is about 8% at 290 K (see Fig. S2). It is interesting to notice that for the ground nanoparticle samples, the percentage of active SCO molecules does not correspond to the obtained enthalpy variation, which suggests also the presence of LS residual fraction at high temperature.

To complete the study, powder X-ray diffractograms for the bulk and film samples before and after increasing the time of grinding were performed at room temperature (Fig. 3).

The general similarities with previously reported data for all measured samples reveal the good composition of the complex and the stability of the SCO complex in the TPU matrix. Although the broadening of the peaks is more pronounced for the starting composite film (certainly due to the strain effect induced by the TPU matrix) in comparison with the starting powder sample, a clear increase of the broadening can be observed only for the ground powder sample, in agreement with the DSC and magnetic measurements revealing defects generated by the grinding of the pure SCO particles. It is also interesting to notice that the relative intensity of the peaks, which differs in the non-ground SCO and composite samples, corroborates a partial orientation of the particles in the composite film. As expected, this difference disappears when increasing the grinding time. For a grinding time of 20 minutes, the relative intensity of the peaks for the film corresponds to that observed for the bulk sample, the latter not varying with grinding time. TEM observations were also carried out for selected powder samples to directly visualize the effect of the grinding on the SCO nanoparticles, showing evolution from rods to an irregular and aggregated morphology (Fig. S3).

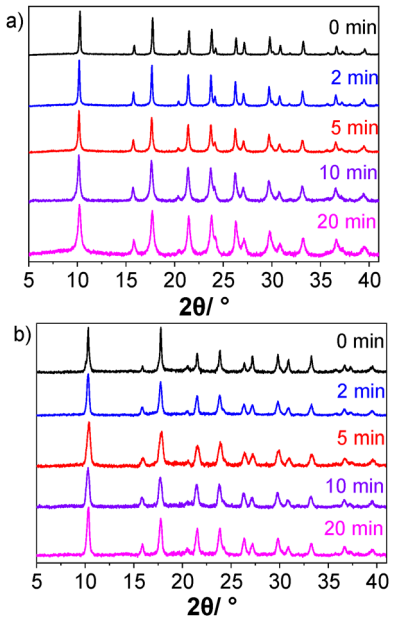

Fig. 3 Powder X-ray diffractograms for the Nps (a) and Nps@TPU films (b) before and after increasing the time of grinding.

In conclusion, the stability of the SCO properties upon grinding was tested and compared for rod-shaped $[Fe(NH_2trz)_3](SO_4)$ particles either "naked" or embedded in a thermoplastic polyurethane matrix. While two minutes grinding of the "naked" nanoparticles was enough to significantly modify the SCO properties with the appearance of a HS residual fraction at low temperature and a less cooperative character, only slight alteration was observed after twenty minutes grinding for the composite film. Thus, the presence of the protective matrix precludes the obliteration of the complete, cooperative and above room temperature SCO properties. Such notable breakthroughs can bolster novel research in the burgeoning field concerning the homogeneous integration of SCO materials into devices made of polymeric based composite materials for various applications.

This project has received funding from the European Research Council (ERC) under the European Union's Horizon 2020 research and innovation program (grant agreement no. 101019522).

Conflicts of interest

There are no conflicts to declare.

Data availability

The data supporting this article have been included as part of the SI. Supplementary information: Mössbauer spectrometry

and transmission electron microscopy. See DOI: https://doi.org/10.1039/d5cc04205d.

References

1 N. P. Bigham and J. J. Wilson, *J. Am. Chem. Soc.*, 2023, **145**(17), 9389–9409.
2 B.-C. Ye, W.-H. Li, X. Zhang, J. Chen, Y. Gao, D. Wang and H. Pan, *Adv. Mater.*, 2024, **36**(45), 2402747.
3 Z. Ul, S. Khan, S. Ullah, H. Ullah, M. U. Khan, M. Ullah and A. A. Altaf, *Crit. Rev. Anal. Chem.*, 2022, **54**(3), 508–528.
4 Y. Yin and J. A. Rogers, *Chem. Rev.*, 2022, **122**(5), 4885–4886.
5 K. S. Kumar and M. Ruben, *Angew. Chem., Int. Ed.*, 2021, **60**(14), 7502–7521.
6 Y. Zhang, R. Torres-Cavanillas, X. Yan, Y. Zeng, M. Jiang, M. Clemente-Leon, E. Coronado and S. Shi, *Chem. Soc. Rev.*, 2024, **53**, 8764–8789.
7 G. Molnár, S. Rat, L. Salmon, W. Nicolazzi and A. Bousseksou, *Adv. Mater.*, 2018, **30**(5), 17003862.
8 K. Ridier, A. Hoblos, S. Calvez, M. Lorencc, W. Nicolazzi, S. Cobo, L. Salmon, L. Routaboul, G. Molnár and A. Bousseksou, *Coord. Chem. Rev.*, 2025, **535**, 216628.
9 M. A. Halcrow, *Dalton Trans.*, 2024, **53**, 13694–13708.
10 S. Kamilya, B. Dey, K. Kaushik, S. Shukla, S. Mehta and A. Mondal, *Chem. Mater.*, 2024, **36**(10), 4889–4915.
11 N. Pittala, F. Thetiot, S. Triki, K. Boukheddaden, G. Chastanet and M. Marchivie, *Chem. Mater.*, 2017, **29**, 490–494.
12 M. Piedrahita-Bello, J. E. Angulo-Cervera, A. Enriquez-Cabrera, G. Molnar, B. Tondu, L. Salmon and A. Bousseksou, *Mater. Horiz.*, 2021, **8**, 3055–3062.
13 R. Torres-Cavanillas, M. Gavara-Edo and E. Coronado, *Adv. Mater.*, 2024, **36**(1), 2307718.
14 K. Ridier, A.-C. Bas, Y. Zhang, L. Routaboul, L. Salmon, G. Molnár, C. Bergaud and A. Bousseksou, *Nat. Commun.*, 2020, **11**, 3611.
15 A. Grosjean, N. Daro, S. Pechev, L. Moulet, C. Etrillard, G. Chastanet and P. Guionneau, *Eur. J. Inorg. Chem.*, 2016, 1961–1966.
16 M. D. Manrique-Juárez, I. Suleimanov, E. M. Hernández, L. Salmon, G. Molnár and A. Bousseksou, *Materials*, 2016, **9**(7), 537.
17 M. S. Haddad, W. D. Federer, M. W. Lynch and D. N. Hendrickson, *J. Am. Chem. Soc.*, 1980, **102**(4), 1468–1470.
18 E. König, G. Ritter, W. Irler and H. A. Goodwin, *J. Am. Chem. Soc.*, 1980, **102**(14), 4681–4687.
19 E. W. Müller, H. Spiering and P. Gütlich, *J. Chem. Phys.*, 1983, **79**, 1439–1443.
20 E. König, G. Ritter and S. K. Kulshreshtha, *Chem. Rev.*, 1985, **85**(3), 219–234.
21 P. J. van Koningsbruggen, Y. Maeda and H. Oshio, *Top. Curr. Chem.*, 2004, **233**, 259–324.
22 M. S. Haddad, W. D. Federer, M. W. Lynch and D. N. Hendrickson, *Inorg. Chem.*, 1981, **20**, 131–139.
23 P. Gutlich and H. A. Goodwin, *Top. Curr. Chem.*, 2004, **233**, 1–47.
24 B. Weber, E. S. Kaps, C. Desplanches and J.-F. Létard, *Eur. J. Inorg. Chem.*, 2008, 2963–2966.
25 J. H. Askew and H. J. Shepherd, *Chem. Commun.*, 2018, **54**, 180.
26 D. Nieto-Castro, F. A. Garces-Pineda, A. Moneo-Corcuera, B. Pato-Doldan, F. Gispert-Guirado, J. Benet-Buchholz and J. R. Galan-Mascaros, *Inorg. Chem.*, 2020, **59**, 7953–7959.
27 J. H. Askew, D. M. Pickup, G. O. Lloyd, A. V. Chadwick and H. J. Shepherd, *Magnetochemistry*, 2020, **6**(3), 44.
28 A. H. Ewald, R. L. Martin, E. Sinn and A. H. White, *Inorg. Chem.*, 1969, **8**(9), 1837–1846.
29 D. C. Fisher and H. G. Drickamer, *J. Phys. Chem.*, 1971, **54**, 4825–4837.
30 P. Gutlich, V. Ksenofontov and A. B. Gaspar, *Coord. Chem. Rev.*, 2005, **249**(17–18), 1811–1829.
31 D. J. Mondal, N. Mukherjee and S. Konar, *Cryst. Growth Des.*, 2023, **23**(3), 1832–1839.
32 R. Li, G. Levchenko, C. Bartual-Murgui, H. Fylymonov, W. Xu, Z. Liu, Q. Li, B. Liu and J. A. Real, *Inorg. Chem.*, 2024, **63**(2), 1214–1224.
33 Y. Garcia, V. Ksenofontov, G. G. Levchenko, G. Schmitt and P. Gütlich, *J. Phys. Chem. B*, 2000, **104**, 5045–5048.
34 L. Salmon and L. Catala, *C. R. Chimie*, 2018, **21**(12), 1230–1269.
35 A. Enriquez-Cabrera, A. Rapakousiou, M. Piedrahita-Bello, G. Molnár, L. Salmon and A. Bousseksou, *Coord. Chem. Rev.*, 2020, **419**, 213396.
36 Y.-H. Luo, H. Dong, S.-H. Ma, F.-L. Zeng, X.-T. Jin and M. Liu, *J. Mater. Chem. A*, 2023, **11**, 1232–1238.
37 D. Nieto-Castro, F. A. Garcés-Pineda, A. Moneo-Corcuera, I. Sánchez-Molina and J. R. Galán-Mascarós, *Adv. Funct. Mater.*, 2021, **31**(33), 2102469.
38 Y. Zan, M. Piedrahita-Bello, S. E. Alavi, G. Molnár, B. Tondu, L. Salmon and A. Bousseksou, *Adv. Intell. Syst.*, 2023, **5**(6), 2200432.
39 H. Voisin, C. Aimé, A. Vallée, T. Coradin and C. Roux, *Inorg. Chem. Front.*, 2018, **5**, 2140–2147.
40 Y. Raza, F. Volatron, S. Moldovan, O. Ersen, V. Huc, C. Martini, F. Brisset, A. Gloter, O. Stéphan, A. Bousseksou, L. Catala and T. Mallah, *Chem. Commun.*, 2011, **47**, 11501–11503.
41 L. Stoleriu, P. Chakraborty, A. Hauser, A. Stancu and C. Enachescu, *Phys. Rev. B: Condens. Matter Mater. Phys.*, 2011, **84**, 132105.
42 A. Tokarev, J. Long, Y. Guari, J. Larionova, F. Quignard, P. Agulhon, M. Robitzer, G. Molnar, L. Salmon and A. Bousseksou, *New J. Chem.*, 2013, **37**, 3420–3432.